

BlinkRadar: Non-Intrusive Driver Eye-Blink Detection with UWB Radar

Jingyang Hu*, Hongbo Jiang*, Daibo Liu*, Zhu Xiao*, Schahram Dustdar[†], Jiangchuan Liu[‡], Geyong Min[§].

*College of Computer Science and Electronic Engineering, Hunan University

[†]Computer Science heading the Research Division of Distributed Systems, Vienna University of Technology

[‡]School of Computing Science, Simon Fraser University

[§]College of Engineering, Mathematics and Physical Sciences, University of Exeter

Email: {fbhhjy, hongbojiang, dbliu, zhxiao}@hnu.edu.cn, dustdar@dsg.tuwien.ac.at, jcliu@cs.sfu.ca, g.min@exeter.ac.uk

Abstract—The eye-blink pattern is crucial for drowsy driving diagnostics, which has become an increasingly serious social issue. However, traditional methods (e.g., with EOG, camera, wearable and acoustic sensors) are less applicable to real-life scenarios due to the disharmony between user-friendliness, monitoring accuracy, and privacy-preserving. In this work, we design and implement BlinkRadar as a low-cost and contact-free system to conduct fine-grained eye-blink monitoring in a driving situation using a customized impulse-radio ultra-wideband (IR-UWB) radar which has superior spatial resolution with the ultra-wide bandwidth. BlinkRadar leverages an IR-UWB radar to achieve contact-free sensing, and it fully exploits the complex radar signal for data augmentation. BlinkRadar aims to single out the eye-blink induced waveforms modulated by body movements and vehicle status. It solves the serious interference caused by the unique characteristics of blinking (i.e., subtle, sparse and non-periodic) and from the human target itself and surrounding objects. We evaluate BlinkRadar in a laboratory environment and during actual road testing. Experimental results show that BlinkRadar can achieve robust performance of drowsy driving with a median detection accuracy of 92.2% and eye blink detection of 95.5%.

Index Terms—Eye Blink detection, RFID Signal, Drowsy driving detection

I. INTRODUCTION

Drowsy driving is a main reason for traffic accidents, resulting in heavy casualties and economic loss, and it has become an increasingly serious problem around the world. Under the state of drowsiness, a driver could significantly reduce vigilance and slow reaction time. According to the U.S. National Highway Traffic Safety Administration, from just 2015 to 2020, over 4121 traffic accidents are related to drowsy driving in the United States [1]. In Europe, statistics [2] show that around 20% of all traffic accidents are due to a diminished vigilance level of drivers caused by drowsiness. Researches on traffic safety [3] show that eye-blink pattern is distinctive when drivers become drowsy, which causes observable physiological phenomenon, i.e., drawn-out eyelid closure. It is therefore crucial to develop a driving state diagnosis system, that can accurately monitor eye-blink motion in driving situation to prevent traffic accidents and save peoples lives.

Traditionally, to monitor such physiological phenomenon for driving state diagnosis, existing eye-blink detection methods mainly rely on different types of sensors, which can be divided into four categories: EOG sensor [4], proximity sensor [5]- [6], camera [7] and acoustic sensor. However, these

systems are less applicable to real-life scenarios due to the disharmony between user-friendliness, detection accuracy, and privacy preserving. Specifically, EOG and proximity sensors are usually embedded in wearable devices such as virtual reality headsets and eye-wears [6]. Although these systems can achieve high detection accuracy, the inconvenience caused by the contact (even intrusive) nature of these sensors has prevented them from being widely adopted under daily driving situations. Unlike EOG and proximity sensors, cameras are usually deployed to capture images or record videos to detect eye-blink motion in a non-intrusive way [8]. Though promising, the performance of camera-based systems degrades in low lighting conditions and may raise privacy concerns, hindering their wide application. With inherent non-intrusive and good privacy-preserved attributes, acoustic sensing, gained a tremendous amount of attention in recent years, shows fantastic potential for eye-blink detection owing to its low propagation speed and wide availability, however, limited by the acoustic wavelength and bandwidth, acoustic-based systems can be susceptible to real-life acoustic interference and with coarse-grained spatial resolution [9]. Because it's a matter of life and death, eye-blink detection should be with high accuracy.

Ideally, in-vehicle eye-blink detection system should be performed continuously with a low-cost (boosting wide application) and potential vehicle-mounted (i.e., in non-intrusive manner) device, providing high detection accuracy and assuring privacy preserving, so that eye-blink patterns can be easily used as markers for intervention or evidence for drowsiness diagnoses [10]. To achieve this goal, inspired by the superior performance of impulse-radio ultra-wideband (IR-UWB) radar in recognizing the motion of an object at a distance, in this work, for the first time, we propose BlinkRadar to employ IR-UWB for RF-based eye-blink motion sensing by harmonizing these crucial concerns on user-friendliness, accuracy detection, and privacy preserving. The principle behind BlinkRadar is that the movements of target object can affect the propagation of IR-UWB signal by reflecting and mingling with raw motion-induced changing patterns embedded with fine-grained spatial information. By actively emitting well-designed IR-UWB signals through a commercial-grade IR-UWB radar platform and analyze how eye-blink motion is modulated in the complex reflection signals.

Although promising progress has been achieved in using IR-UWB for wireless sensing, eye-blink detection still faces the following challenges. First, eye-blink motion is extremely subtle. Compared with respiratory sensing that monitors the chest displacement of about 5 mm, the eyelid has a thickness of as low as 0.5 mm [11]. The subtle displacement and limited reflection area-caused signal variation is so small that can be easily buried in background noise. Hence, identifying eye-blink waveform with RF-sensing is far from trivial even for static subjects, not to mention the highly dynamic driving situations. Moreover, the reflected signals bounced off the eyes and other in-car activities (e.g., body and respiratory movements, driving and road vibrations, etc) are mixed together, making it extremely hard to detect eye-blink from these interferences. Third, eye-blink is a sparse motion in time domain with aperiodicity and markedly variable blink interval (ranging from hundreds of ms to tens of seconds). These properties make frequency domain analysis and model-based methods infeasible for eye-blink detection.

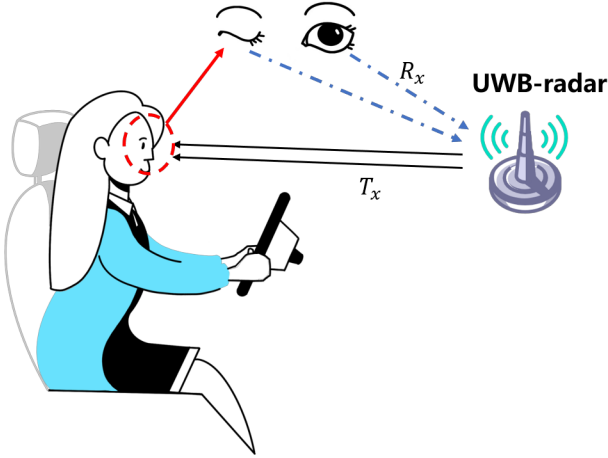


Fig. 1: COTS impulse radio used in BlinkRadar and radio setup inside the vehicle.

To tackle these challenges, we design BlinkRadar the first RF-based non-intrusive, fine-grained and motion-robust eye-blink detection system. We implement BlinkRadar based on a commercial-grade IR-UWB radar platform [12], leveraging its large bandwidth (e.g., as high as 1.5GHz) to achieve high-resolution (i.e., 1.5cm) motion sensing. Given the raw eye-blink-induced IR-UWB signal embedded with fine-grained spatial information, we distill the subtle motion of eye-blink by analyzing different transformations induced by actions at different positions in the in-phase and quadrature (I/Q) vector space. Based on the characteristics of I/Q-domain signal representation, we further analyze the impact of fine-grained motion change of eye-blinking on the signal change of both amplitude and phase, i.e., the movement of eyelids (open and close eye) can affect the RF transmission path modally and contributing to characterized phase change; due to the different reflection factor of eyelid and the eyeball, the presence and absence of eyelids can lead to different amplitude of reflected signals. Given these signal features caused by eye-blink, we

design an algorithm to detect eye blink.

To summarize, our contributions are as follows.

- To the best of our knowledge, BlinkRadar is the first RF-based non-intrusive, fine-grained and motion-robust eye-blink detection system operating in a commercial-grade IR-UWB radar platform.
- We analyze the necessity to process radar signal in its complex I/Q domain, on this basis leveraging the phase or amplitude of the signal. We propose using the unique variation of the signal in the I/Q vector space for recovering and refining eye-blink waveform, which fully utilizes the I/Q components together and achieves fine-grained eye-blink waveform recovery leveraging the generalizability brought.
- We conduct extensive evaluations and field studies to evaluate the performance of BlinkRadar. The results strongly confirm its excellent performance in eye-blink detection under driving situation. It can achieve median detection accuracy of 95.5% of eye blink detection and 92.2% of drowsy driving detection. BlinkRadar is robust to various unfavourable factors, including bumpy road and sunglasses-wearing of the driver.

The rest of this paper is organized as follows. Section II presents the feasibility analysis of applying RF signals for eye-blink sensing. Section III introduces the system overview. Section IV present the whole system. Section V presents the implementation of BlinkRadar. Section VI presents the system evaluation. Section VIII discussed the limitation of our work. By discussing the related works in Section VII, we conclude this work.

II. FEASIBILITY ANALYSIS

In this section, we first verify whether blinking can generate a response through a valid RF signal. We then explore the unique motion of signal changes due to the blink signal, and in this section, we conduct extensive empirical studies that inspire us to advance this work. Before the feasibility analysis, We need to understand the pattern of blinking when drowsy.

A. Eye-Blink Pattern during Drowsy Driving

Eyes blink a physical need. When blinking, the tears can evenly wet the cornea and conjunctiva so that the eyeball will not be dry, keep the cornea lustre, and remove the conjunctival sac dust and bacteria. If you don't blink, the tear film on the eyeball will quickly evaporate, and we will feel dry, uncomfortable, stinging, and teary eyes. Considering the caffier's study [11], the typical eye-blink duration is less than 400ms on average and 75ms for the minimum. When a person enters an exhausted state, the blinking time will exceed 400ms or even longer. We monitor the driver by monitoring the driver's long-term blinking time to know the driver's blinking time length change during driving to monitor the driver Driving state.

B. The Motion of Eye-Blink

Eye-blink has the characteristics of non-periodic and sparseness, human blink has a unique movement pattern. We first introduce the movement pattern of the human eye and then

introduce the relationship between blink movement and signal changes. To explore the unique signal changes produced by eye-blinks, we placed the UWB radar 30 cm in front of the participants' eyes. As shown in Fig. 2(a), UWB radar receives the signal reflected from the eye and transfers the signal into I-Q space to analyze the phase and amplitude variation pattern of the signal. To distinguish the signal changes during blinking, we divide the blinking process into two stages, Eye Closing Stage and Eye Opening Stage.

Eye closing stage. When closed eyes, the human eyelid will reflect the RF signal, and the path of the reflected signal will change from the eyeball to the receiving antenna to the eyelid to the receiving antenna. This will produce subtle path changes, which will lead to changes in the signal phase. Meanwhile, the surface of the eyeball and the eyelid are different reflectors, and reflectors of different materials have different signal reflectivity, so the signal reflected from the surface of the eyeball and the eyelid will have different manifestations in amplitude. The specific process as shown in Fig. 2(b)

Eye opening stage. When the eyes are opened, the process is opposite to closing the eyes. As shown in Fig. 2(b), we see that in the IQ space, the amplitude of the signal becomes smaller when the eye is opened, and the phase of the signal is The opposite change. We can separate the blink-related signal from the multipath-filled signal through this extraordinary signal feature change.

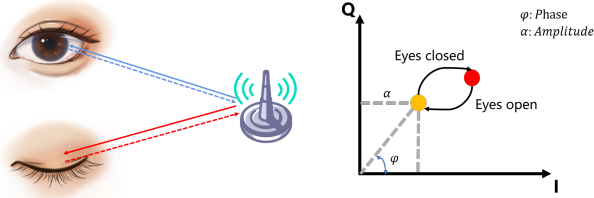


Fig. 2: The Schematic diagram of UWB radar and I-Q space.

C. Blink Frequency When Drowsy

To demonstrate the relationship between drowsiness and blink frequency, we recruited 8 participants to qualitatively test changes in blink time when they were tired and not tired. We tested it at 10:00 in the morning and night when everyone was in their best spirits. At 10:00, participants determined they were in a state of fatigue and then performed an eye-blink test. We used blink frequency to indicate whether participants were drowsy [13]. To ensure the reliability of the survey and empirical testing, light conditions were kept constant (i.e., 220 260 lux light intensity), and the distance between participants and the device was always kept constant (30 cm).

For simplicity and without loss of generality, we plotted their 1-minute blinks in a table when they were energized and lethargic. I. We found that participants blinked more often when tired than when they were energized.

TABLE I: Blink frequency at different times

	1	2	4	5	6	7	8
10:00am	20	21	19	20	18	22	21
10:00pm	25	26	30	25	26	24	26

III. SYSTEM OVERVIEW

This section introduces the overview of BlinkRadar. The whole system consists of three components: signal preprocessing, Eye-blink detection, and Drowsy driving detection.

Signal preprocessing. In this model, We introduced the signal preprocessing process of BlinkRadar. This module includes noise reduction and background subtraction. The UWB radar transmits a signal, and the signal is reflected and received by the radar receiving end again. At the same time, the data is transmitted to the computer for processing. We want to use a smoothing filter to reduce the noise in the signal, and then we use a loopback filter to remove static reflections from the clutter for background subtraction.

Eye-blink detection. This model introduces how to extract the blink signal from the mixed signal. We first convert the received signal to the IQ space. We analyze the unique signal pattern changes caused by blinking, including changes in signal amplitude and phase. Then we introduced how to find the best blink observation position and remove the noise caused by vehicle vibration. Since the human body cannot maintain a posture, the human body will move slightly, and the surrounding environment will also change. Therefore, BlinkRadar needs to update the viewing position adaptively in real-time to maintain good blink detection performance. We have designed an algorithm that can continuously update the best observation position.

Drowsy driving detection. This part of the model introduces how to continuously perform blink detection in a moving car. Drowsy driving is mainly reflected in the driver's blink rate and blink time. We designed a drowsy detection algorithm and recruited participants to conduct experiments. In order to verify BlinkRadar, we collected the blink rate and blinked time of the participants when they were sleepy and awake. We verified the feasibility of BlinkRadar in the onboard drowsiness detection system through cross-validation.

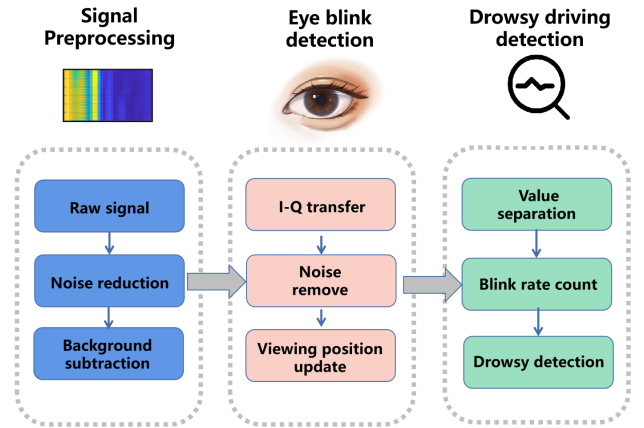


Fig. 3: Overview of BlinkRadar design.

IV. SYSTEM DESIGN

A. RF Signal Design

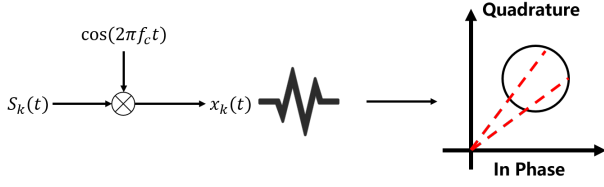


Fig. 4: Signal preprocessing process.

In this section, we introduce the design of RF signal design of the UWB radar. BlinkRadar utilizes a system-on-chip impulse radio for transmitting and receiving wireless pulses. The schematic diagram of transmitting signal and receiving signal is shown in Fig. 4. The transmitted signal is $s_k(t)$, the modulated signal is $x_k(t)$, the signal after passing the channel is $y_k(t)$, and the demodulated signal is $y_k^b(t)$. The receiving end receives in-phase and Quadrature (IQ) sampling at the receiver side for downconversion.

The COST UWB radar we use combines the transmitting antenna with the receiving antenna. The transmitting antenna continuously sends out chirp signals and the receiving antenna will receive echoes. The transmitted chirp can be represented as

$$s(t) = V_{tx} \exp\left(-\frac{(t - \frac{T_p}{2})^2}{2\sigma_p^2}\right) \quad (1)$$

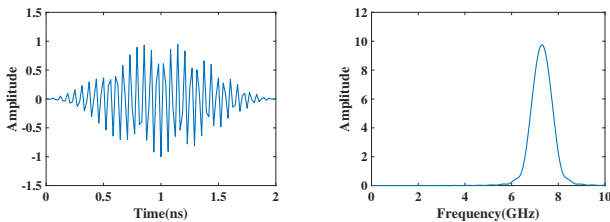
where the V_{tx} is the amplitude of the pulse, the duration of the signal is T_p and σ_p^2 is the variance corresponding to the -10 dB bandwidth. We employ an in-phase single-carrier frequency $\cos(2\pi f_c t)$ for upconversion. Then, the transmitted signal in time domain is given by:

$$x_k(t) = s(t - kT_s) \cdot \cos(2\pi f_c(t - kT_s)) \quad (2)$$

where f_c is carrier frequency, T_s is duration of frame, k denotes the k -th frame. Because the impulse radio transmits a sequence of identical pulses, we have $s(t - kT_s) = s(t)$. So the equation can be written as:

$$x_k(t) = s(t) \cdot \cos(2\pi f_c(t - kT_s)) \quad (3)$$

The carrier frequency of the signal is 7.3GHz and the bandwidth is 1.4GHz. The transmitted signal $x_k(t)$ is shown in the Fig. 5(a) and the Spectrogram of the $x_k(t)$ is illustrated in Fig. 5(b).



(a) Transmitted $x_k(t)$ in time domain (b) Transmitted $x_k(t)$ in frequency domain
Fig. 5: The time and frequency domain of transmitted signal

The impulse response $h_k(t)$ is given by:

$$h_k(t) = \sum_{p=1}^P \alpha_p \delta(t - \tau_p - \tau_p^D(kT_s)) \quad (4)$$

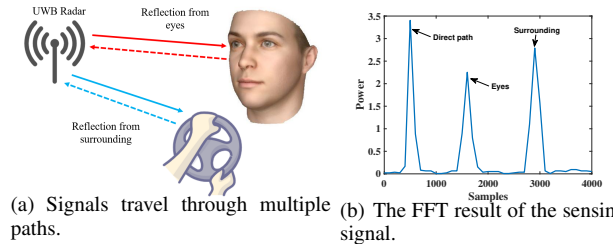
where α_p is the channel gain of the p^{th} reflection path signal in the vehicle, τ_p is the time delay of the p -th path, $\tau_p^D(kT_s)$ is the time delay caused by Doppler frequency shift of the p -th path. The $\tau_p = \frac{2R_p}{c}$ and $\tau_p^D(kT_s) = \frac{2v_p kT_s}{c}$, Where R_p is the distance between the target to the UWB radio. c is the speed of electromagnetic wave, v_p is the speed of the moving target. The range resolution of Blink Radar is $\Delta r = \frac{c}{2B}$. The received signal of the system is:

$$y_k(t) = h_k(t) * x_k(t) \quad (5)$$

Received baseband signal $y_k^b(t)$ are obtained after applying IQ space, we have:

$$y_k^b(t) = \sum_{p=1}^P \alpha_p e^{2\pi f_c(\tau_p + \tau_p^D(kT_s))} \cdot s(t - kT_s - \tau_p - \tau_p^D(kT_s)) + n(t) \quad (6)$$

For common pulse radar, we can use two-dimensional fast Fourier transform for ranging and speed measurement processing, we will receive the signal for (FFT), we can get different objects at different distances relative to UWB radar, As shown in Fig. 6(b). We have seen three Peaks corresponding to different signal paths. The first path is the path directly received by the antenna itself, the second is the path reflected from the eye, and the third is the path reflected from the environment. We further divide the signal path into a static path and a dynamic path. All static path signals, including direct path signals and reflections from static surrounding objects. We denote the superimposed composite signal as H_c where H_c is a vector summation of H_s and H_d . For most small-scale movements, the amplitude of the dynamic vector can be assumed as a constant and only the phase changes. Therefore, the dynamic vector rotates with respect to the static vector, inducing the signal variations in the I-Q vector space.



(a) Signals travel through multiple paths. (b) The FFT result of the sensing signal.
Fig. 6: The illustration of eye-blink detection in a multipath environment, and the corresponding ToFs (frequency shifts) of the multiple paths, respectively.

B. Rf Signal Preprocessing

Before extracting information from RF signals, the effects from hardware or environment should be removed to guarantee signal quality. The RF signals preprocessing has two main steps: i) noise reduction and ii) background subtraction.

1) *Noise reduction*: The received baseband signals are polluted with noise, as shown in Fig. 8(a). Noise will prevent the following vital signs extraction modules to work properly. Especially, vital signs will be immersed in noise. Therefore, a cascading filter comprised of a low-pass Finite Impulse Response (FIR) filter and a smoothing filter are utilized to enhance the SNR of the signals. The order of the designed FIR filter is 26 and Hamming window is used. The smooth filter with a window size of 50 points is used to further smooth the output signal of the FIR filter. Fig. 8(b). illustrates the output of the cascading filter. It can be seen that noise is suppressed.

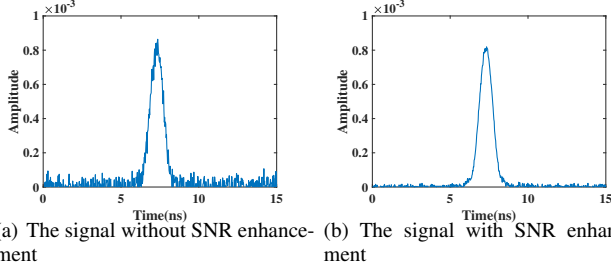


Fig. 7: The signal without SNR enhancement and with SNR enhancement

2) *Background subtraction*: BlinkRadar needs to remove reflections from other objects. Each reflector in the vehicle produces a reflected component in the overall signal, and this component has a frequency shift that is linearly related to the reflected time-of-flight. For example, reflections from the seats and steering wheel are much stronger than reflections from the eyes. These reflections can interfere with blink detection.

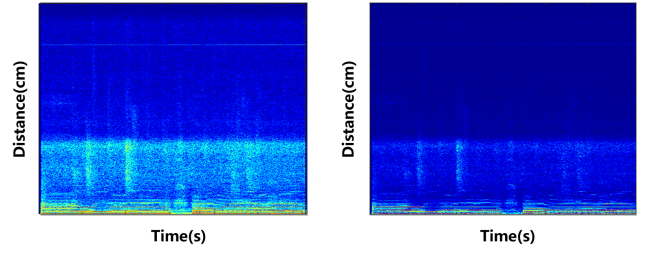
To remove reflections from all these static objects (seats, steering wheel), we take advantage of the fact that since these reflectors are static, their distance from the UWB radar are not time-dependent, so the frequency shift they cause remains constant over time. We take an FFT of the received signal for each scan window and calculate the power at each frequency as a function of time. Note that there is a linear relationship between the two. The frequency shift and distance traveled are as follows:

$$distance = C \times TOF = C \times \frac{\Delta f}{slope} \quad (7)$$

We can use the equation above to plot the power reflected from each distance as a function of time. As shown in Fig. 8(a), we can see from the picture that there are many static components similar to straight lines, and their energy does not change with time. Therefore, we remove the power of these static reflectors from the FFT scan of the signal in the previous scan by simply subtracting the output of the given FFT. This process is called background subtraction because it removes all static reflectors in the background. The result after elimination is shown in Fig. 8(b).

C. Eye-Blink Motion Capture

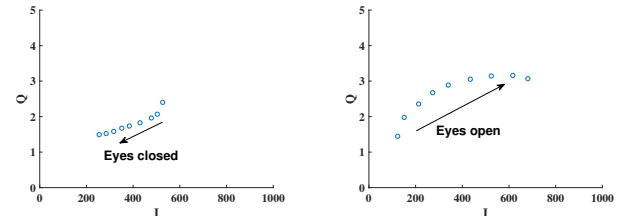
Though human blinks are aperiodic and sparse, human blinks have unique movement patterns. We first introduce the movement patterns of the human eye, and then introduce the



(a) Signal before background subtraction. (b) Signal after background subtraction.
Fig. 8: The signal without background subtraction and with background subtraction

relationship between blink movement and signal changes. We introduce this relationship in Sec.3, and we now present actual experimental results.

The change of the signal in the IQ space in the closed eye phase is shown in Fig. 9(a). We observed that the signal's amplitude becomes small, this change is since the surface of the eyeball and the eyelid's surface are different reflectors. The reflectors of different materials have different signal reflectivity, so the signal reflected from the eyeball's surface and the eyelid's surface will have different performance in amplitude. At the same time, the reflection path of the signal changes, and the reflection signal changes from eyelid reflex to eyeball reflex. Results in a change in the phase of the signal. The process of opening the eyes is the opposite of closing the eyes. As shown in Fig. 9(b), we observe that the signal amplitude becomes large, and the phase also changes accordingly. We can distinguish this unique pattern from the blink-related signal from the multipath fill signal.



(a) The signal variation of Eyes closed (b) The signal variation of Eyes open

Fig. 9: The signal variation of Eyes closed and open

Through the previous results, we can summarize the effect of the blinking process on the signal as to when blinking occurs. The signal transmission path will slightly change, and the signal amplitude will change due to the difference in the reflection of the signal by the eyelid and eyeball. In the I-Q space, the amplitude of the signal can be expressed as

$$\varphi = -2\pi(f_0\tau - \frac{B}{2T}\tau^2) \quad (8)$$

In the blink of an eye, The value of $\frac{B}{2T}\tau^2$ can be ignored, the $\tau = \frac{2d}{c}$, we denote The change of phase $\Delta\varphi$ as

$$\Delta\varphi = -\frac{4\pi f_0 \Delta d}{c} \quad (9)$$

The signal phase change can be represented by $\Delta\varphi$. The Changes in signal amplitude can be used $\Delta\alpha$. We record blinks

by capturing the changes in the phase and amplitude of the unique signal during blinking in the I-Q space.

D. Eyes Blink signal extraction

This section will introduce how BlinkRadar filters out blink-related signals from the multiple noises. Before we introduce how to remove these noises, we first need to understand them and how they affect BlinkRadar.

Multiple noise. The sensing signals will travel through multiple paths from the transmitter to the receiver. Signals reflected from surrounding objects are called ambient interference. Environmental disturbances can come from static objects, such as seats and steering wheels, or from moving objects, such as fidgeting passengers. In addition to the signals reflected from the eyes, there are also signals reflected from other parts of the body. Interference caused by signals reflected from other parts of the body is called self-interference. Such as the head when yawning, the hands when operating the steering wheel.

Biosignal noise. Faces and the human body produce biosignals that interfere with our blink detection. These biological signals include heartbeat and breathing. The movement of the heartbeat is small but will maintain a stable cycle. At the same time, the heartbeat information will be hidden in the breathing information. Many studies have shown that the chest cavity will be displaced by 3-5cm when breathing. At the same time, the head moves involuntarily when breathing, and there is an approximate 1mm head movement that is synchronized with the heartbeat due to the pumping of blood, which is called Ballistic Cardiography (BCG). This involuntary movement is aliased with blinking information. Different from ambient noise, this type of noise embedded in the blinking information is more difficult to remove.

To solve Multiple noise and Biosignal noise. We mainly use two methods to solve and help us extract the information from blinking.

The signal separation. To coarsely separate the blink signal from the noise which is easier to separate, we first use the chirp signal. UWB radar will continuously transmit pulse signals with carrier frequency of 7.3GHz and bandwidth of 1.4GHz. The speed of the electromagnetic wave c is 3.0×10^8 , the resolution of RF signal with a bandwidth of 1.4GHz is able to distinguish two signals with a distance difference larger than 1.07 cm. The resolution of 1.07cm helps us easily separate the signal from the blink of the eye from the motion of the driver's limbs and chest, and we design filters to filter out unwanted noise in the environment. But the movements of the driver's face, including the movement of the lips, and the involuntary small-amplitude movements of the head can be mixed into the blink signal. A finer-grained signal separation is required to obtain a clean blink signal.

Fine-grained blink features. Since both breathing and heartbeat are periodic motions, the induced involuntary head movements are also periodic. The motion of the head is clearly different from blinking in the I-Q space. As shown in Fig. 10(a). We use blue for head movement and yellow for blink movement. Signal amplitude changes caused by small head displacements (approximately 1mm) are negligible, while

the corresponding phase changes are significant. So if we don't consider the static vector, the phase change causes the dynamic vector to rotate relative to the origin, and since the amplitude change is negligible, the radius of the arc is approximately constant.

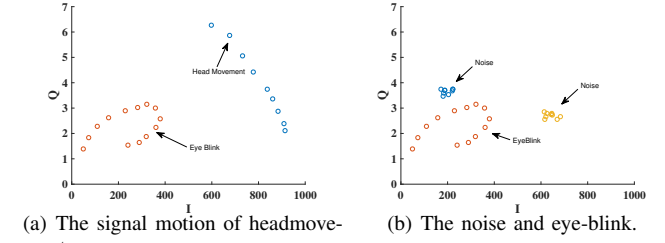


Fig. 10: The signal motion of headmovement and the noise and eye-blink.

When we apply the chirp signal design to eye-blink detection in a multipath environment, reflectors at different distances cause different amounts of frequency shift, and the signals fall into different frequency bins. After performing FFT on the sensed signal (mixed signal). We can get multiple reflectors located at different frequencies corresponding to different frequency ranges. Without prior knowledge of the distance between the eye and the sensing device, when there are multiple peaks, we do not know which peak corresponds to the eye reflection signal. The naive approach is to differentiate the ocular reflection signal by distinguishing the amplitude of the peaks. However, due to the small reflection area, the magnitude of eye reflections may be weaker than reflections from other surrounding objects such as steering wheels and seats, even if the eye is closer to the sensing device.

To quickly identify the frequency bins corresponding to the eyes, we exploited the disturbances caused by respiration and heartbeat, rather than relying directly on the signal changes caused by blinking. The reason is that blinking is a sparse activity, with blink intervals ranging from a few seconds to tens of seconds, which may If we identify the frequency bins of eye reflexes by blinking, a large delay is introduced. In contrast, embedded interference persists even without blinking, which can be used to quickly identify frequency bins of eye reflections. Illustrates the signal changes in the frequency of the eye's reflections when the eye is not blinking. We have an interesting observation: while the 1D amplitude variation of the eye-reflected signal is small, the signal in the 2D I-Q vector space varies greatly, forming arc-shaped trajectories due to embedded disturbances. As shown in Fig. 10(b), the eye reflection frequency can be easily distinguished from the noise in 2D space. Therefore, to identify the frequency bins corresponding to the eyes, we first calculate the variance of the 2D signal variation for each frequency bin, and then pick out the frequency bins with the largest variance. Note that this is the first time we've exploited "harmful" embedded interference to aid our blink-sensing signal processing.

E. Real-time Eye-Blink Detection

Although the above viewing position scheme can achieve good blink detection performance, the optimal Observe po-

sition changes during long-term detection due to slight body movement of the target and changes in the surrounding environment. Therefore, we need to adaptively update the viewing position in real time to maintain good sensing performance. Since we obtained the optimal viewing position by the arc fitting method, the more signal samples we have, the more accurate the optimal viewing position. However, more data samples means greater system latency and can impact real-time performance. Below, we present the design details of our real-time algorithm to maintain a good balance between detection accuracy and system.

Signal transmission and reception. In the beginning, our system collects several signal samples for the initialization. Specifically, we accumulate 50 chirps with the default chirp period of 40mm, which takes 2s in total. Note that this 2s is for the cold-start and is a one-time effort. Once the system is initiated, we can output the detection results every 40mm. Therefore, our proposed system can provide real-time detection. We apply the well-known Pratt method for the arc fitting, which is lightweight and robust.

Extreme value separation After obtaining the best viewing position, BlinkRadar continuously tracks the relative distance from the viewing position to the newly collected signal samples. Since the blink cycle takes 100 400mm. We apply a local extreme value detection (LEVD) method to detect the bumps caused by blinks in a sliding window. The basic idea of the LEVD method is to find alternative local maxima and minima and compare the difference between two nearby local maxima and minima with a predefined threshold. Set to five times the standard deviation of the signal amplitude without blinking. A blink is detected if the local maximum and minimum difference is more significant than a threshold.

Adaptive update. During the driving process of the vehicle, the vibration of the vehicle body and the adjustment of the driver's posture will change the distance between the eyes and the UWB radar, so BlinkRadar needs to update the observation position constantly. Since the optimal view position calculation is very lightweight, we continuously. The viewing position is updated as soon as enough samples are accumulated. Note that if too few samples are used For arc fitting, the accuracy can be pretty low. BlinkRadar restarts the whole eye-blink detection process when a significant body movement happens. BlinkRadar constantly finds the best viewing position, through which it can continuously capture the blinking action.

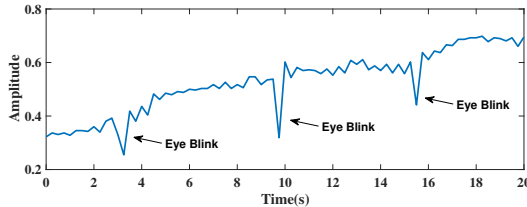


Fig. 11: An illustrative example of our real-time eye-blink detection algorithm.

F. Drowsy Driving Detection

In this section, We'll introduce how BlinkRadar performs drowsy driving detection.

BlinkRadar aims to detect whether a user has entered a drowsy state by detecting their blink rate, and we now discuss the rationale behind our approach. When the user is very awake and driving with full attention, the user's eyes will look ahead to observe the road conditions, and the blinking frequency will remain normal. When the user enters a sleepy state, the blink rate becomes higher. Previous research has shown that when users feel drowsy in the initial stages, the blink time is longer, and the blink rate is higher. Although not a contribution of our work, for the integrity of drowsy driving detection. We built a model to verify that we can do this reliably. We build a simple model for drowsy driving detection based on the above description.

We use blinkTime to denote blink duration, decided by the 1st and the last sample of consecutive closed eyes. Then, The blink rate denote the frequency of blink. To unify units, BlinkRate is the frequency of blinks per minute. Finally, we define

Mild drowsy=(BlinkTime>8000ms)|| (BlinkRate>0.3)

Severe drowsy=(BlinkTime>1600ms)|| (BlinkRate>0.4)

Next, we built a separate machine learning model for each. The model includes two scenarios: awake, drowsy. We use a one-minute window to calculate the user's blink rate, and we collect each user's blink rate while awake and drowsy and leave one Cross-validation method to validate our algorithm.

V. IMPLEMENTATION

Hardware implementations. BlinkRadar performs eye-blink detection identification using UWB signals. The core component is a compact, low-cost Novelda X4M05 [55] IR-UWB transceiver. They are used to transmit and receive RF signals for eye-blink sensing. The sampling frequency is 23.328GHz, and we set the frame per second as 400. The radio is connected to a Raspberry Pi via Serial Peripheral Interface (SPI). The hardware PCB is relatively small with a size of 6.5 3cm². The hardware includes a power supply, 5V fan, Raspberry Pi, and impulse radio. We place the whole uwb radar on the windshield of a vehicle. Since the impulse radio is facing the driver The eye-blink detection modules are implemented using Python 3.7 and PyTorch 1.7.1. All code will be executed on an MSI laptop (GTX 1060 graphics card and I7-7700).

Signal parameters. It transmits a baseband signal with a bandwidth of 1.5GHz, and the signal is further modulated onto a 7.29GHz carrier.

Ground truth. We employ a separate smartphone as the recording device to record the ground truth using the camera. The recording device is held by an adjustable tripod and placed at the same height as the sensing device. We first collected two sets of data for each participant, blinking data while awake at 10:00 am in a stationary vehicle and then drowsy at 10:00 pm. The blink data at the time, these two data sets are used as the training set. In order to maintain the safety of the experiment, we choose to conduct the experiment when the

driver is awake, and the experiment is carried out in an open area with sparse traffic. The driver does not enter the drowsy state. We will have the experimenter give instructions to the participants. When the typical driving instruction is given, the driver blinks according to the regular pattern, and when the drowsy instruction is given, the driver drives. Participants will be asked to blink to simulate their drowsiness blinking pattern.

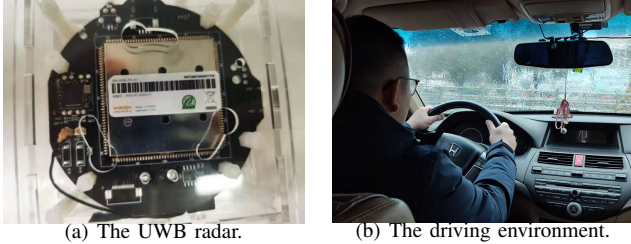


Fig. 12: The UWB radar and driving environment.

VI. EVALUTAIION

In this section, we comprehensively evaluate the performance of BlinkRadar using the UWB Radar by varying the parameters under different conditions. Our extensive experiments on actual vehicles and the road demonstrate the potential of BlinkRadar for practical use of drowsy driving detection using wireless signals.

A. Experiment Setup

To verify the performance of BlinkRadar, we recruited 12 participants (8 male and 4 female). Their ages ranged from (19 to 27). We used a Volkswagen Sagitar as an experimental vehicle. We study the influence of different factors by arranging UWB radar on the front window and changing the parameters and conditions. We collected data for each driver in the vehicle when they were awake and asleep. Then to simulate actual driving, we will ask the participants to drive on the road at a uniform speed (road at night, with low traffic volume). We will not ask the participants to reach a state of drowsiness while driving but will give instructions to ask them. The data were collected while driving by simulating their blinking patterns when fee drowsy.

B. Overall Performance

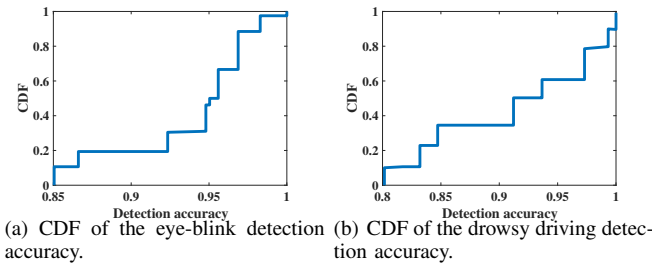


Fig. 13: CDF of the detection accuracy.

BlinkRadar mainly performs two functions, one is blink detection, and the other is drowsy driving detection based on blink detection. We first explore the overall blink detection performance and drowsy driving detection performance.

Accuracy of eye-blink detection. The accuracy of blink detection is defined as the number of correctly detected eye-blinks over the total number of eye-blinks. As show in Fig. 13(a), The overall median accuracy of eye-blink detection can reach 95.5%.

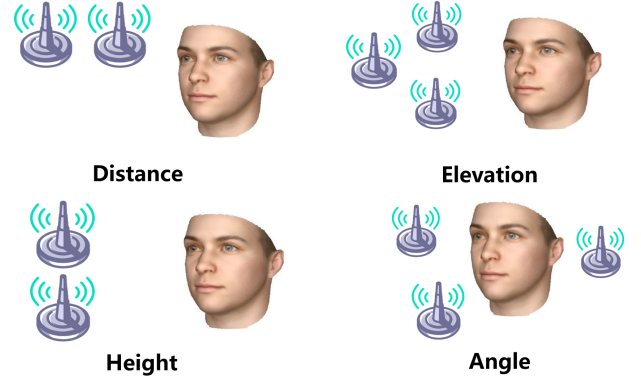


Fig. 14: Illustration of different relative positions of the sensing device with respect to the human target.

Accuracy of drowsy driving detection. The accuracy of drowsy driving detection is defined as the number of correctly detected drowsy driving over the total number of drowsy driving. As show in Fig. 13(b), The overall median accuracy of drowsy driving detection can reach 92.2%. Next, we transform the parameters to study the factors that affect the detection accuracy of BlinkRadar.

C. Continuous Blink Missed Detection Rate

To verify the stability of BlinkRadar, we examine the continuous missed detection rate of BlinkRadar during the continuous blink detection process. The experimental results are shown in the figure. The first missed detection rate in continuous blink detection is 4.9%, the probability of two consecutive missed detections is 2.1%, and three consecutive missed detections are 0.2% as shown in Fig. 15(a). The results prove that BlinkRadar can be stably used for blink detection.

D. Distance from UWB Radar to Participant

UWB radars are placed at different distances of 20, 40, and 80cm, respectively. Its direction Eyes are facing the human target. We can achieve a detection accuracy that exceeds 95% in 40 cm as shon in Fig. 15(b). When the distance increases to 80 cm, the accuracy drops to 91%. Therefore, We advise keeping the device within 0.4 m for high accuracy.

E. Elevation and height from UWB radar to participant

The sensing device is placed at different heights from 0 degrees to 60 degrees in steps of 15 spend. The sensing device is placed facing the eye of the human target. we define the user's line of sight is 0 degrees, We can see that performance decreases with height increase as shown in Fig. 15(c). Within 30 degrees, BlinkRadar can achieve a high detection accuracy of 95%.

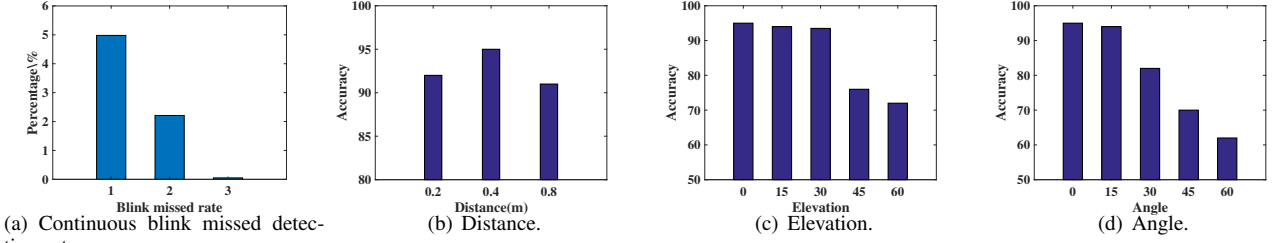


Fig. 15: Illustration of continuous blink missed detection rate and different relative positions of the sensing device with respect to the human target.

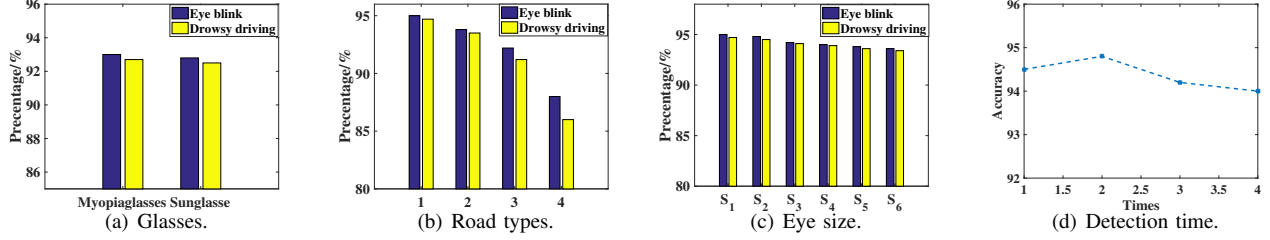


Fig. 16: Other factors.

F. Angle from UWB Radar to Participant

We positioned the UWB radar to face the participant's eyes at 0 degrees. We tested the detection performance of BlinkRadar in the range of 0 degrees to 60 degrees with a step size of 15 degrees, and the result is as shown in Fig. 15(d). It can be seen that in the range of 0 degrees to 15 degrees, BlinkRadar can maintain more than 90% detection accuracy. When the angle is more significant than 30 degrees, the detection accuracy drops significantly, which may be related to the angle of the antenna being too far away from the participant.

G. Impact of Glasses

Considering the ubiquity of glasses wearers, BlinkRadar needs to complete blink detection under the premise that users wear glasses. We mainly evaluate two types of glasses (myopia glasses and sunglasses). We fixed the UWB radar to the front of the windshield. Fig. 16(a) shows that the detection accuracy of BlinkRadar is 94% and 93%, respectively. Although the accuracy rate is slightly lower than when the glasses are not worn, the system can still complete the routine work. Blink detection in the case of wearing glasses and wearable devices is also our next work direction.

H. Impact of Road Types and Traffic Conditions

The signal quality of BlinkRadar can be affected by different road types and traffic conditions, thus affecting the performance of BlinkRadar. Make sure that BlinkRadar works on different road types and different traffic conditions. We collect data on different road types (e.g. smooth highway, bumpy road, uphill road, downhill road, intersection, left turn, right turn, roundabout, U-turn) and analyze the results separately. The result is shown in Fig. 16(b). It can be seen that if the road surface is smooth and the number of manoeuvres is small, the estimation error of blink detection is low, during the bumpy

road surface and Driving manoeuvres can increase estimation error.

I. Impact of Eye Size

Different users have different eye sizes. We want to know whether the size of the user's eyes will affect the performance of BlinkRadar, and we give the detection accuracy of each of them according to the size of the user's eyeballs. We found that the user's eye size does affect the detection as shown in Fig. 16(c), but even with the smallest eye size in the experiment (3.5 x 0.8cm), BlinkRadar still maintains more than 90% accuracy.

J. Impact of Detection Time

Fig. 16(d) shows the accuracy of drowsy driving detection under different detection windows. It can be seen that when the time length is between 1min and 2min, BlinkRadar can achieve the highest detection accuracy. Too short a detection window detects too few samples. Too long a detection window is easy to delay the detection of drowsy driving. We set BlinkRadar's drowsy detection window to 1min.

VII. RELATED WORK

This section briefly introduces the literature background related to blinking detection and some wireless sensing-based driving behaviour detection. Blink detection currently mainly includes detection schemes based on wearable devices and detection schemes based on cameras. The detection scheme based on wearable devices mainly acquires the information of blinking action through sensors deployed around the eyes. Camera-based detection schemes detect blinks by recording the user's face and using image processing techniques. The driving actions detection based on wireless sensing includes drowsy driving actions, distracted driving actions, and the detection of the driver's breathing and heartbeat. Below we will introduce some practical cases.

A. Eye-Blink Detection Methods

1) *EOG-based blink detection*: Electrooculography (EOG) sensors are the most widely used method for eye tracking and blink detection. Andreas et al. [14] describe the design, implementation and evaluation of a novel eye tracker for context-awareness and mobile HCI applications. Hiroyuki et al. [15] input interfaces for the severely handicapped and object-of-interest selection in the camera finder. They will bring great benefits when they can be used easily in everyday life. D et al. [16] developed a lab view-based EOG logger to acquire EOG data and subsequently analyze it in MATLAB. Activity status data collection was performed in the early morning with the subjects' consent. Subjects were asked to perform an activity while acquiring the data. Video recordings were also performed simultaneously to verify the performance of the EOG system. Raj et al. [17] using electrodes placed at specific positions around the eyes, are conditioned for detection and analysis of these movements. However, the characteristics of EOG signals obtained substantially depend on the electrode placement.

2) *Wearable device detection methods*: Wearable devices use smart glasses and VR glasses-based methods to combine head movements and eye movements for human activity recognition. Shoya et al. [18] demonstrate how information about eye-blink frequency and head motion patterns derived from Google Glass sensors can be used to distinguish different types of high level activities. Oribits et al. [19] Using an off-the-shelf Jins MEME pair of eyeglasses, present a pilot study that suggests that the eye movement required for Orbits can be sensed using three electrodes. 3D-Spatial [6] investigated the effect of three-dimensional (3D) spatial learning on eye-blink in computer graphics-generated visual environments. Devender et al. [20] describes an Electrooculogram (EOG) and gaze based hands-free natural interaction system design for virtual reality (VR) games which enhances the immersive VR experience.

3) *Camera-based detection methods*: Recently, there have been many methods using Cameras to detect eye-blinks. The camera's low cost, non-contact and easy portability make it the most widely used method for detecting drowsy driving. Taber [21] presents an automatic drowsy driver monitoring and accident prevention system that is based on monitoring the changes in the eye-blink duration. CafeSafe [22] app for Android phones that incorporates information from the front and rear cameras and other embedded sensors on the phone to detect and alert drivers to dangerous driving situations inside and outside the car. However, the method based on the Camera needs to consume a lot of computing power, and using a Camera in the car will cause potential privacy leakage problems. Our proposed method based on UWB radar consumes less computing power and does not cause privacy leakage problems.

B. Driving Action Detection Methods

Existing works exploit biological features including EEG (electroencephalogram) and PPG (photoplethysmogram) to detect fatigue driving. Li et al. proposed a PPG sensor

based driver fatigue detection method [23], and Dkhil et al. introduced a EEG based fatigue index based on alpha spindles [24]. Balasubramanian et al. employed the signal power in the 15-30 Hz frequency band for muscle fatigue detection [25]. Biological features form the basis for directly reflecting the fatigue state of the driver. However, these methods rely on complex and expensive equipment and therefore are difficult to be widely adopted.

Drowsy and distracted driving detection systems based on wireless sensing have seen significant development recently. ER [26] realized an early warning system which detects inattentive events. D^3 -Guard [27] utilized the Doppler shift of acoustic signals to capture the driver's action patterns to detect drowsy driving. DriverSonar [28] Detects dangerous driving actions using unique acoustic echo information. CARIN [29] used CSI-based technology to recognize activity of passenger in the presence of interference. Recently, Zhang et al. designed a diffraction-based sensing model to recognize exercises and daily activities using WiFi signals [30]. Moreover, Wi-Fi Radar [31] and V2ifi [32] were proposed to use RF signal to detect human activity.

VIII. DISCUSSION

In this section, we discuss the limitations of our system and potential future work.

A. Limitation

We expect BlinkRadar to be as perfect as possible, but in fact, BlinkRadar is flawed. Compared with traditional camera-based solutions, BlinkRadar is more strict about placement. Traditional camera-based schemes can start performing blink detection as long as the human eye can be captured in the footage. After our research, there are two main reasons for this limitation.

The limited angular range of the antenna. The angle range of the camera is mainly 45 degrees. However, for BlinkRadar, when the angle of the antenna exceeds 30 degrees, the detection performance will drop significantly. At the same time, the range of the human eye is petite, and the reflected energy is fragile, so the angle of reflection of the antenna is more stringent.

Complex road conditions and body vibration. In a moving car, the performance of the system degrades as we continue to drive over rough roads. The reason is that vibration and displacement can change the distance measurement between the UWB radar and the human body, thus affecting the sensing performance. Equipment vibration/displacement. This is a real challenge for wireless sensing because the detected motion information comes from both the target and the device. It is not easy to separate them to get target information.

In conclusion, we propose incorporating BlinkRadar into the perception method of drowsy driving as a camera-based alternative in scenarios where users have high privacy requirements.

IX. CONCLUSION

In this paper, we implement a subtle blink detection platform using RF signals on IR-UWB Through theoretical

and experimental analysis, We quantitatively modeled the relationship between signal changes and subtle eye-induced movements blinks. In this work, we design and implement a low-cost and contactless drowsy driving detection system that strikes a balance between user-friendliness, monitoring accuracy, and privacy protection.. Comprehensive experimental results Demonstrate the effectiveness of our system. We evaluate BlinkRadar during laboratory environments and real-world road tests. Experimental results show that BlinkRadar can achieve robust performance with a median detection accuracy of 95%.

REFERENCES

- [1] "Us drowsy-driving traffic accidents," <https://www.nhtsa.gov/risky-driving/drowsy-driving>, 2017.
- [2] "Us distracted-driving traffic accidents," <https://www.nhtsa.gov/risky-driving/distracted-driving>, 2018.
- [3] G. Sikander and S. Anwar, "Driver fatigue detection systems: A review," *IEEE Transactions on Intelligent Transportation Systems*, vol. 20, no. 6, pp. 2339–2352, 2019.
- [4] M. S. Reddy, B. Narasimha, E. Suresh, and K. S. Rao, "Analysis of eog signals using wavelet transform for detecting eye blinks," in *2010 International Conference on Wireless Communications Signal Processing (WCSP)*, 2010, pp. 1–4.
- [5] —, "Analysis of eog signals using wavelet transform for detecting eye blinks," in *2010 International Conference on Wireless Communications & Signal Processing (WCSP)*. IEEE, 2010, pp. 1–4.
- [6] M. Takao, T. Ishiguro, T. Kubota, and M. Iijima, "3d-spatial learning and eye blink," in *2019 IEEE 1st Global Conference on Life Sciences and Technologies (LifeTech)*, 2019, pp. 283–285.
- [7] A. Kuwahara, R. Hirakawa, H. Kawano, K. Nakashi, and Y. Nakatoh, "Eye fatigue prediction system using blink detection based on eye image," in *2021 IEEE International Conference on Consumer Electronics (ICCE)*, 2021, pp. 1–3.
- [8] C.-W. You, N. D. Lane, F. Chen, R. Wang, Z. Chen, T. J. Bao, M. Montes-de Oca, Y. Cheng, M. Lin, L. Torresani, and A. T. Campbell, "Carsafe app: Alerting drowsy and distracted drivers using dual cameras on smartphones," in *Proceeding of the 11th Annual International Conference on Mobile Systems, Applications, and Services*, ser. MobiSys '13. New York, NY, USA: Association for Computing Machinery, 2013, p. 1326. [Online]. Available: <https://doi.org/10.1145/2462456.2465428>
- [9] J. Liu, D. Li, L. Wang, and J. Xiong, "Blinklistener: "listen" to your eye blink using your smartphone," *Proc. ACM Interact. Mob. Wearable Ubiquitous Technol.*, vol. 5, no. 2, jun 2021. [Online]. Available: <https://doi.org/10.1145/3463521>
- [10] C. Xu, Y. Zheng, and Z. Wang, "Efficient eye states detection in real-time for drowsy driving monitoring system," in *2008 International Conference on Information and Automation*, 2008, pp. 170–174.
- [11] P. P. Caffier, U. Erdmann, and P. Ullsperger, "The spontaneous eye-blink as sleepiness indicator in patients with obstructive sleep apnoea syndrome-a pilot study," *Sleep Medicine*, vol. 6, no. 2, pp. 155–162, 2005.
- [12] T. Zheng, Z. Chen, C. Cai, J. Luo, and X. Zhang, "V2ifi: in-vehicle vital sign monitoring via compact rf sensing," *Proceedings of the ACM on Interactive, Mobile, Wearable and Ubiquitous Technologies*, vol. 4, no. 2, pp. 1–27, 2020.
- [13] P. Ren, X. Ma, W. Lai, M. Zhang, S. Liu, Y. Wang, M. Li, D. Ma, Y. Dong, Y. He, and X. Xu, "Comparison of the use of blink rate and blink rate variability for mental state recognition," *IEEE Transactions on Neural Systems and Rehabilitation Engineering*, vol. 27, no. 5, pp. 867–875, 2019.
- [14] A. Bulling, D. Roggen, and G. Tröster, "It's in your eyes: Towards context-awareness and mobile hci using wearable eog goggles," ser. UbiComp '08. New York, NY, USA: Association for Computing Machinery, 2008, p. 383384. [Online]. Available: <https://doi.org/10.1145/2578153.2583039>
- [15] H. Manabe and T. Yagi, "Eog-based eye gesture input with audio staging," ser. ETRA '14. New York, NY, USA: Association for Computing Machinery, 2014, p. 8493. [Online]. Available: <https://doi.org/10.1145/1409635.1409647>
- [16] D. Suman, M. Malini, and S. Anchuri, "Eog based vigilance monitoring system," in *2015 Annual IEEE India Conference (INDICON)*, 2015, pp. 1–6.
- [17] R. Anchan, A. Pillay, A. Kale, A. Bhadriraja, and S. P. Ram, "Optimal bipolar lead placement in electrooculography (eog): A comparative study with an emphasis on prolonged blinks," in *2020 11th International Conference on Computing, Communication and Networking Technologies (ICCCNT)*, 2020, pp. 1–7.
- [18] S. Ishimaru, K. Kunze, K. Kise, J. Weppner, A. Dengel, P. Lukowicz, and A. Bulling, "In the blink of an eye: Combining head motion and eye blink frequency for activity recognition with google glass," in *Proceedings of the 5th Augmented Human International Conference*, ser. AH '14. New York, NY, USA: Association for Computing Machinery, 2014. [Online]. Available: <https://doi.org/10.1145/2582051.2582066>
- [19] M. Dhuliawala, J. Lee, J. Shimizu, A. Bulling, K. Kunze, T. Starner, and W. Woo, "Smooth eye movement interaction using eog glasses," in *Proceedings of the 18th ACM International Conference on Multimodal Interaction*, ser. ICMI '16. New York, NY, USA: Association for Computing Machinery, 2016, p. 307311. [Online]. Available: <https://doi.org/10.1145/2993148.2993181>
- [20] D. Kumar and A. Sharma, "Electrooculogram-based virtual reality game control using blink detection and gaze calibration," in *2016 International Conference on Advances in Computing, Communications and Informatics (ICACCI)*, 2016, pp. 2358–2362.
- [21] T. Danisman, I. M. Bilasco, C. Djeraba, and N. Ihaddadene, "Drowsy driver detection system using eye blink patterns," in *2010 International Conference on Machine and Web Intelligence*, 2010, pp. 230–233.
- [22] C.-W. You, M. Montes-de Oca, T. J. Bao, N. D. Lane, H. Lu, G. Cardone, L. Torresani, and A. T. Campbell, "Carsafe: A driver safety app that detects dangerous driving behavior using dual-cameras on smartphones," in *Proceedings of the 2012 ACM Conference on Ubiquitous Computing*, ser. UbiComp '12. New York, NY, USA: Association for Computing Machinery, 2012, p. 671672. [Online]. Available: <https://doi.org/10.1145/2370216.2370360>
- [23] G. Li and W.-Y. Chung, "Detection of driver drowsiness using wavelet analysis of heart rate variability and a support vector machine classifier," *Sensors*, vol. 13, pp. 16494–16511, 2013.
- [24] A. W. M. B. Dkhil and A. M. Alimi, "Drowsy driver detection by eeg analysis using fast fourier transform," in *2015 15th International Conference on Intelligent Systems Design and Applications (ISDA)*, ser. ISDA '16, 2016, pp. pp. 313–318.
- [25] V. Balasubramanian and K. Adalarasu, "Emg-based analysis of change in muscle activity during simulated driving," *J. Bodywork Movement Therapies.*, vol. 11, pp. 151–158, 2017.
- [26] X. Xu, H. Gao, J. Yu, Y. Chen, Y. Zhu, G. Xue, and M. Li, "Er: Early recognition of inattentive driving leveraging audio devices on smartphones," in *IEEE INFOCOM 2017 - IEEE Conference on Computer Communications*, 2017, pp. 1–9.
- [27] Y. Xie, F. Li, Y. Wu, S. Yang, and Y. Wang, "D3-guard: Acoustic-based drowsy driving detection using smartphones," in *IEEE INFOCOM 2019 - IEEE Conference on Computer Communications*, 2019, pp. 1225–1233.
- [28] H. Jiang, J. Hu, D. Liu, J. Xiong, and M. Cai, "Driversonar: Fine-grained dangerous driving detection using active sonar," *Proc. ACM Interact. Mob. Wearable Ubiquitous Technol.*, vol. 5, no. 3, sep 2021. [Online]. Available: <https://doi.org/10.1145/3478084>
- [29] Y. Bai and X. Wang, "Carin: Wireless csi-based driver activity recognition under the interference of passengers," *Proc. ACM Interact. Mob. Wearable Ubiquitous Technol.*, vol. 4, no. 1, Mar. 2020. [Online]. Available: <https://doi.org/10.1145/3380992>
- [30] F. Zhang, K. Niu, J. Xiong, B. Jin, T. Gu, Y. Jiang, and D. Zhang, "Towards a diffraction-based sensing approach on human activity recognition," *Proc. ACM Interact. Mob. Wearable Ubiquitous Technol.*, vol. 3, no. 1, Mar. 2019. [Online]. Available: <https://doi.org/10.1145/3314420>
- [31] Y. Zou, W. Liu, K. Wu, and L. M. Ni, "Wi-fi radar: Recognizing human behavior with commodity wi-fi," *IEEE Communications Magazine*, vol. 55, no. 10, pp. 105–111, 2017.
- [32] T. Zheng, Z. Chen, C. Cai, J. Luo, and X. Zhang, "V2ifi: In-vehicle vital sign monitoring via compact rf sensing," *Proc. ACM Interact. Mob. Wearable Ubiquitous Technol.*, vol. 4, no. 2, 2020.